HIGH BRIGHTNESS BEAM MEASUREMENT TECHNIQUES AND ANALYSIS AT SPARC

D. Filippetto *, M. Bellaveglia, E. Chiadroni, A. Gallo, LNF-INFN, Frascati, Italy,
A. Mostacci, Università La Sapienza, Roma, Italy
A. Cianchi, B. Marchetti, INFN-Roma II, Roma, Italy
C. Ronsivalle, ENEA C.R. Frascati, Frascati, Italy

Abstract

Ultra-short electron bunch production is attractive for a large number of applications ranging from short wavelength free electron lasers (FEL), THz radiation production, linear colliders and plasma wake field accelerators. SPARC is a test facility able to accelerate high brightness beam from RF guns up to 150MeV allowing a wide range of beam physics experiments. Those experiments require detailed beam measurements and careful data analysis. In this paper we discuss the techniques currently used in our machine; by combining quadrupoles, RF deflector, spectrometer dipole and reliable data analysis codes, we manage to characterize the 6D phase space and the beam slice properties. We focus on the ongoing studies on the emittance compensation in the velocity bunching regime.

INTRODUCTION

High energy (150MeV) beam measurements at SPARC are performed by means of a quadrupole triplet, a RF deflector and a spectrometer magnet downstream from the third accelerating section. The transverse beam size is measured on the flags F_1, F_2, F_3, holding a YAG screen each, for different values of current in quadrupoles Q_T1, Q_T2, Q_T3 and in the spectrometer and/or deflecting voltages (see Fig. 1).

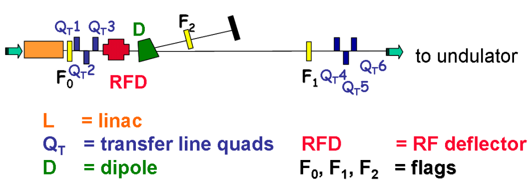

Figure 1: Layout of the high-energy experimental area.

BEAM IMAGE ANALYSIS

Most of the main properties of high brightness beam can be inferred by the evolution of beam sizes under particular conditions. At SPARC (and in many FELs) such properties are measured with fluorescent screens intercepting the beam; the beam transverse footprint is then digitalized with CCDs after proper optical manipulations. The resulting images has to be (automatically) analyzed to distinguish the beam signal from the background noise (e.g. dark current, x-rays, . . .).

* Daniele.Filippetto@lnf.infn.it

The noise can be correlated or uncorrelated with the presence of beam signal. A typical example of the uncorrelated noise is the dark current hitting on the detection screen. On the contrary, reflections at the screen borders or relevant x-rays signals usually come with electron beam. Another problem in noise treatment are the pixel value fluctuations, given by the background light fluctuations and by the noise on the readout electronics. Each pixel can have a background level different from the other ones (for construction errors), which can be divided by a mean level (correlated noise) superimposed to frame-by-frame fluctuations (uncorrelated noise), the amplitude of both depending on the gain in the readout chain. Correlated noise can be strongly reduced with average background subtraction

Other noise filtering are usually more complicated, since they must be performed automatically and as much as possible independently from the user analyzing the data. Roughly the noise reduction techniques can be divided in two classes depending if they are applied to the image profile or to the full two dimension image.

The profile based filtering is most suited for broad and low level signals. In this case the signal appear as a big correlated halo, with maximum value of the same order of the background fluctuations. While it could be difficult to automatically and precisely isolate the borders of the signal working on the full image (2D matrix), for example comparing pixel neighbors, it is relatively simpler if working with profiles. By integrating the image in a given direction on a plane, the low and broad signal sums up linearly, differently from the statistical noise whose fluctuation amplitude sums with the square root of the number of integrated pixels.

On the contrary, the two dimension image analysis may be more complicated but it allows a better result in all the other cases, typically when the beam signal is very narrow but very high, i.e. with a small total area, but high local intensity.

Another advantage of the two dimension analysis is the efficiency in denoising. In this case the signal can be perfectly shaped around the noise, from any direction. Instead, in the profile based filtering one looses information since the noise fluctuation along the direction of integration could not be separated from the signal.

In this paper we will focus on the two dimension image analysis; interested reader can find a profile noise reduction technique in Ref. [2].

The main steps of the analysis are:

1 **average background subtraction**. An equal number

of signal and background images (by closing the laser shutter) are acquired; thus an average background image is subtracted from each acquired beam image, in order to remove the correlated noise. The average background image indeed has the uncorrelated noise strongly reduced by the operation of mean, leaving the correlated noise untouched (mean pixel background level).

2 **selection of a region of interest**. The operator interactively chooses one region of interest on an image being the sum of all the beam images. This step is mandatory to remove the noise correlated to the presence of the beam (e.g. reflection on the screen borders).

3 **creation of a mask covering the region where the signal is present**. This is the most critical step: the borders of the beam have to be precisely identified since its RMS dimensions strongly depend on the tails, therefore a small variation in applied cut leads to big differences in RMS size. The algorithm is based on a $N_s \times N_s$ pixels sub-matrix scanning the selected region of interest, eliminating every structure smaller than its dimensions, while leaving untouched all the bigger structures (similar to the "*erode and dilate*" concept of image processing) . The sub-matrix dimension N_s has to be chosen carefully, given the imaging system magnification and the smaller beam dimensions possible. Such a mask is usually computed on the average signal image to keep the computation time reasonable; in special cases, the jitter in the beam position is not negligible, this last step is applied to each acquired beam image. A typical case at SPARC is the high sensitivity energy measurement.

Once that the beam footprint has been recovered from the image, the RMS beam size σ in each transverse direction is computed directly from the profile: being I_j the height of the profile at the j-position and I_{tot} the profile area,

$$\sigma = \sqrt{\sum_{j=1}^{N} \frac{I_j}{I_{tot}} (j-m)^2} \quad \text{with} \quad m = \sum_{j=1}^{N} j I_j. \qquad (1)$$

Such a quantity is extremely sensitive to noise far from the profile centroid m; therefore image analysis is crucial in any beam measurement relying on beam size measurement.

An example of a typical noise reduction is reported in Fig. 2 from a bunch length measurement in the laser comb experiment at SPARC [3] where the distance between beam initially spaced 6ps can be varied via velocity bunching. The left picture is the image after average background subtraction (with the light reflection on the YAG screen border clearly visible), while the right picture shows the result after denoising performed on the full two dimension image automatically.

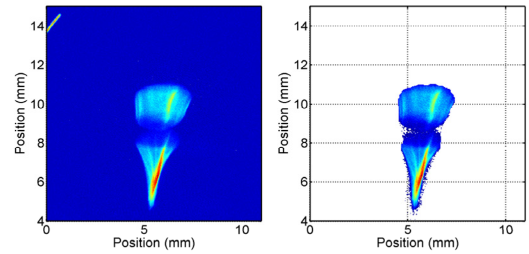

Figure 2: Beam transverse image after a RF deflector in the comb beam experiment at SPARC [3] (200pC, 100MeV).

In the velocity bunching experiment recently performed at SPARC [1], the bunch length has been reduced from the nominal size to about a factor 14. Figure 3 shows two beam footprints after two slightly different beam image (automatic) analysis (left column) for the maximum compression case (i.e. smaller bunch length). The corresponding vertical profiles are reported in the right column pictures: the violet curves are the profiles of the image after the background subtraction, while the dashed curves are the profile used in the RMS size calculation.

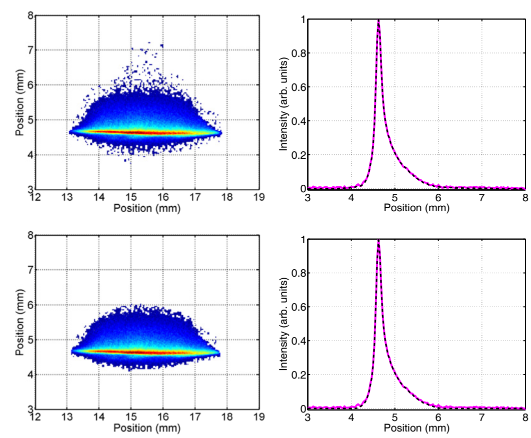

Figure 3: Image analysis in a bunch length measurement in a velocity bunching experiment [1] at SPARC for a 200fs beam (300pC, 100MeV).

At least for this kind of beams, it is clear how the RMS size concept itself is intrinsically questionable from the experimental point of view, since it is strongly affected by small difference in the image analysis. In Table , we consider the two analysis reported in Fig. 3 on the same beam image, labeling "First analysis" ("Second analysis") the one concerning the upper (lower) pictures.

The difference in charge between the two analysis is 2.7% in the considered case, while the difference in RMS sizes is almost 20%. This big difference is due to the strong dependence of the RMS on the tails of the distribution which have been cut differently in the two above analysis.

Table 1: Comparison Among Different Definitions of Beam Size

	First an.	Second an.	diff.
Signal area (arb. un.)	110888	107870	2.7%
RMS size (μm)	328	263.1	19.8%
Gaussian fit (μm)	157.5	157.3	0
FWHM size (μm)	102.1	102.13	0
HWGA size (μm)	207.1	199.5	3.6%

The RMS definition is very useful for beam distributions close to Gaussian, but could be questionable otherwise. In Table have been reported beam dimensions calculated with other possible different size definitions. The second line reports the results of a Gaussian fit. The difference in this case is negligible, but the goodness of fit is clearly very poor, and thus the value not reliable. The Full Width Half Maximum (FWHM) is also stable by definition respect to the tail treatment. On the other hand it does not contain any information on the percent of charge included in it and therefore it may not be useful to determine the beam quality. For example two beams with very different brightness can have similar FWHM.

The last definition discussed is called Half Width at Gaussian Area. It gives half width of the part of the distribution including the 68.2% of the total charge (to compare with the RMS of a Gaussian distribution). This value changes between the two analysis by roughly the same amount of the charge estimation. HWGA size is stable by changing filtering algorithm, contains exact information on the contained charge, and collapse on the RMS value for Gaussian beams.

The previous analysis pretend to take the 100% of beam charge, i.e. including halos. Beam halos affect the measured beam emittance and they can be estimated measuring the emittance for different levels of charge cut. The pixels of each denoised beam image are ordered with a weight function W_j:

$$W_j = \frac{I_j}{(\frac{x_j-\overline{x}}{\sigma_x})^2 + (\frac{y_j-\overline{y}}{\sigma_y})^2}, \qquad (2)$$

where x_j (y_j) is the position of the j-th pixel of intensity I_j and $\overline{x}$ ($\overline{y}$) is the beam centroid in x (y), while σ_x (σ_y) is the horizontal (veritcal) RMS dimension. The cut starts from the pixels with smaller weights, until the desired percent in charge is reached.

BEAM MEASUREMENTS

The image analysis allows retrieving beam centroid position and transverse size. By measuring them after various beam manipulations, it is possible to measure longitudinal and transverse emittance, longitudinal phase space and bunch length using the elements shown in the layout of Fig. 1. In the SPARC case emittance measurement are performed with single and double quadrupole scan [4]; the bunch length is measured with a S-band RF deflector which can give also the longitudinal phase space if used with the spectrometer dipole [5]. Slice measurement are also possible using the RF deflector during a quadrupole scan (horizontal slice emittance) and during an energy measurement (slice energy spread).

As an example we discuss some implications of the above discussed image denoising in the SPARC projected emittance measurements.

The presence of beam halos can affect the emittance measurement, i.e. the emittance of the core beam can be overestimated if considering only the full charge emittance measurement. By changing the percentage of the image area considered for the RMS size evaluation (as discussed in the previous section), one can quantify the effect of the charge halos on the emittance value, as reported in Fig. 4. The left picture shows a gun solenoid scan for a 300pC beam to find the working point of minimum emittance in a typical SPARC operation. The right picture shows the minimum emittance (i.e. at 158A) as a function of the charge cut. The deviation from the linear dependency in the emittance versus charge curve shows the presence of halos. In the particular case of Fig. 4 at least a 10% charge beam halo is present. Selecting the 80% of the beam results in a emittance reduction by a factor of two.

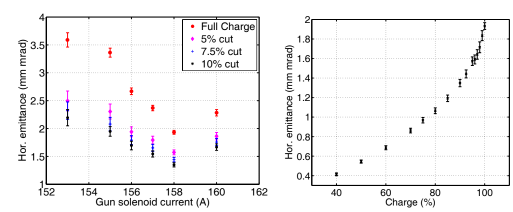

Figure 4: Emittance as a function of the charge cut for a gun solenoid scan (300pC, 150MeV).

CONCLUSION

In this paper, we have discussed some data analysis issues concerning measurement on ultra short, high brightness electron beams. Advanced 2D image denoising procedure is needed to perform non questionable measurement. We have discussed a possible algorithm, showing some practical implications in length measurement of velocity bunched beam. We have shown also how such analysis allows to estimate the effect of beam halos on quadrupole scan emittance measurement.

REFERENCES

[1] M. Ferrario *et al.*, Phys. Rev. Lett. 104, 054801 (2010).

[2] A. Mostacci *et al.*, Rev. Sci. Inst. 79, 013303 (2008).

[3] M. Ferrario *et al.*, Proc. of IPAC10, TUPE082 (2010).

[4] E. Chiadroni *et al.*, Proc. of DIPAC09, 402-404 (2009).

[5] D. Alesini *et al.*, Nucl. Instr. Meth. A, 568, 488-502 (2006).